Heliyon 6 (2020) e04124

Contents lists available at ScienceDirect

Heliyon

journal homepage: www.cell.com/heliyon

Research article

Electrochemical investigations of DNA-Intercalation potency of bisnitrophenoxy compounds with different alkyl chain lengths

Maria Shakeel [a], Tehmeena Maryum Butt [a], Maria Zubair [a], Humaira Masood Siddiqi [a,**], Naveed Kauser Janjua [a,*], Zareen Akhter [a], Azra Yaqub [a,b], Sadia Mahmood [a]

[a] Department of Chemistry, Quaid-i-Azam University, Islamabad, 45320, Pakistan
[b] Chemistry Division, Directorate of Science, Pakistan Institute of Nuclear Science and Technology (PINSTECH), P.O. Nilore, Islamabad, 45650, Pakistan

ARTICLE INFO

Keywords:
Electrochemistry
Materials science
Cyclic voltammetry
Bisnitrophenoxy compounds
Methylene spacer length
dsDNA intercalation

ABSTRACT

In this study, the binding tendency of bisnitrophenoxy compounds (BN) having different methylene $(–CH_2–)_n$ spacer groups (n = 8–11) with fish sperm double stranded deoxyribonucleic acid (dsDNA) was explored. Cyclic voltammetry (CV) was used to evaluate various kinetic and binding parameters ($K_{s,h}$, D_o, K_b and binding site sizes). Performed electrochemical studies designated strong contact of these symmetric molecules with dsDNA in threading intercalation mode of binding. The number (n) of methylene spacer group in the molecular structure of bisnitrophenoxy compounds, e.g., BN-8 (1-nitro-4-(8-(4-nitrophenoxy)octyloxy)benzene, was observed to have a strong influence on their binding affinity. Decreased peak current values and positively shifted peak potentials recorded *via* cyclic voltammetry clearly depicted that bisnitrophenoxy compounds can intercalate with dsDNA. Results demonstrated the following order of binding constants; K_b (M^{-1}): BN-8 (2.32×10^4) < BN-9 (5.73×10^4) < BN-10 (8.97×10^4) < BN-11 (17.34×10^4). The order of increasing binding sites from BN-8 (0.13) to BN-11 (1.38), revealed the maximum threading intercalation strength by bisnitrophenoxy compound having the longest methylene spacer (n = 11). Thermodynamic studies augmented the strong binding of BN-11 with dsDNA as compared to BN-8 because of the long-chain, $–CH_2$- spacer in its structure. The spontaneity of dsDNA-binding was revealed by the negative ΔG values for interaction of all the compounds. Moreover, binding parameters from thermodynamic and kinetic studies also corresponded to the threading intercalation mode of interaction, which itself points to the potency of the envisioned drug-like molecules.

1. Introduction

Deoxyribonucleic acid (dsDNA) is a structural unit of the living organism that contains all the genetic instructions for their development and functions. Any mutation to a single genomic sequence in dsDNA can cause genetic disorders. dsDNA molecules are susceptible to damage under oxidative condition, where they may act as a free radical or undergo uncontrolled cell division which may cause cancerous abnormalities [1, 2, 3].

Cancer is one of the most deleterious problems of the world. The treatments primarily used for cancer are radiotherapy and chemotherapy. To restrain this perilous disorder in the field of chemotherapy, researchers have more interest in exploring such types of drugs that are less virulent, have greater binding affinity especially with the minor groove of dsDNA and are site distinguishing towards target [4, 5, 6, 7]. Many studies revealed that binding affinities of different drugs are affected by varying the substituent and spacer length in the drugs [8, 9, 10, 11, 12].

Intercalation of drug with DNA occur through two different modes; groove binding or threading intercalation. Intercalators usually have planar aromatic ring that can bind either by electrostatic interaction or Vander wall forces with base pairs of DNA helical structure. Combining two intercalating units with long chain alkyl linkers gives more complex structure, named threading bis-intercalators, have shown better targeted interaction with DNA base pairs [13, 14].

Nitroaromatic compounds have been found to be biologically active and possess antitumor, antimicrobial, antibiotics and anticancer nature [15, 16, 17, 18, 19]. These tremendous activities of nitroaromatic compounds are due to the cytotoxic activity of the radical anions, generated during the metabolic pathways of nitroaromatic compounds [20, 21].

* Corresponding author.
** Corresponding author.
E-mail addresses: humaira_siddiqi@yahoo.com, humairas@qau.edu.pk (H.M. Siddiqi), nkausarjanjua@yahoo.com, nkjanjua@qau.edu.pk (N.K. Janjua).

https://doi.org/10.1016/j.heliyon.2020.e04124
Received 5 September 2019; Received in revised form 6 December 2019; Accepted 29 May 2020

The techniques that have been widely used to study the binding of compounds with dsDNA are spectroscopic methods, nuclear magnetic resonance, isothermal calorimetry, quartz crystal microgravimetry, and electrochemical methods etc. [22, 23, 24, 25, 26, 27]. Electrochemical studies especially cyclic voltammetry (CV) has been proved to be an efficient tool to investigate the binding of nitroaromatic compounds with dsDNA, due to their redox nature [28, 29, 30]. The main pathway involved in the reaction of such species is initiated by the transfer of one electron. The formed radical anion gets protonated and then reduced further. The reduction product that takes part in dsDNA binding can be addressed by using voltammetric analysis, while the protonation is affected by varying the surfactant and the presence of aprotic solvent [29, 31].

We previously investigated the interaction of a range of bisnitrocompounds (N3–N6) with dsDNA, where the binding affinity of the compounds with dsDNA was found to increase with an increase in alkyl chain length within the molecular structure [9]. In contribution to our previous work, in this paper, we report the interacalation of a group of bisnitrophenoxy compounds (BN-8 to BN-11) with dsDNA using cyclic voltammetry and studied the consequence of increasing chain length on binding tendency. The structurally similar bisnitrophenoxy compounds, having different spacer lengths, showed threading mode of binding [32]. The electrokinetic analysis of neat bisnitrophenoxy compounds revealed diffusion-controlled nature of the process. Thus, signifying the dependency of intercalation process on the molecular size.

2. Experimental

The bisnitrophenoxy structures (BN-8 - BN-11) presented in Figure 1 were prepared following the reported method [33]. Commercially available dsDNA extracted from fish sperm was used to assess the interaction of all bisnitrophenoxy compounds. 5 mM solution of each compound was prepared in DMSO/water mixture (80%/20%) with TBAP supporting electrolyte.

2.1. CV measurements

Cyclic voltammetric analysis was performed using Gamry Potentiostat Interface 1000 with glassy carbon (GC) working electrode (active area of 0.07 cm^2) against Ag/AgCl reference with Pt wire as counter electrode.

The solvent background scan was run in the selected potential range of bisnitrophenoxy compounds. All CV profiles were recorded in the inert environment created by purging argon gas to avoid exposure of O_2. In order to compensate the IR/ohmic drop and to uphold the vicinity of working and reference electrode, three-electrode cell configuration was employed. Prior to each measurement, GC was polished and cleaned using fine alumina, later it was thoroughly washed with distilled water followed by the working solvent. As the dsDNA is electrochemically inactive in the potential window of GC, therefore the solutions of these compounds were CV titrated against dsDNA.

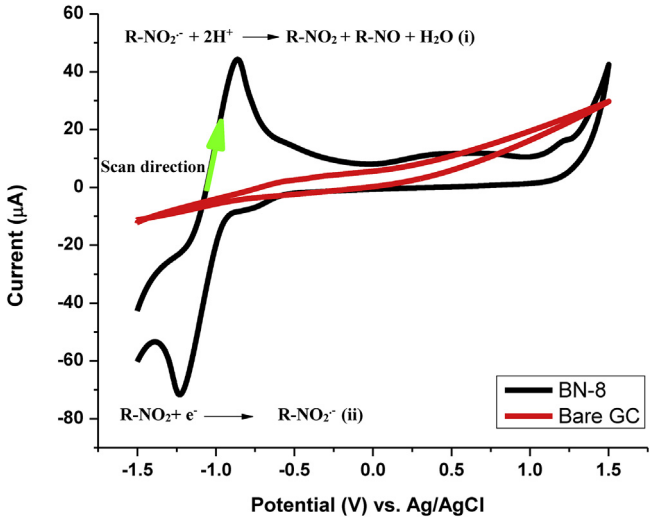

Figure 2. Comparison of voltammogram for solvent background current and bisnitrophenoxy compound (BN-8) in DMSO/water (8:2) mixture at 0.1 V/s.

3. Results

The kinetic parameters and diffusion coefficient values of neat bisnitrophenoxy compounds BN-8 to BN-11) were determined using CV profiles at different sweep rates, afterwards, their intercalation studies with dsDNA was explored by gauging different binding parameters.

3.1. Electrochemical response of neat bisnitrophenoxy compounds

To get an insight of the electrochemical system, electrokinetics and diffusional behavior of pure bisnitrophenoxy compounds with respect to their structural variation, cyclic voltammetric analysis were carried in binary mixture of DMSO and water in potential window of -1.5–1.5 V at 298 K under argon.

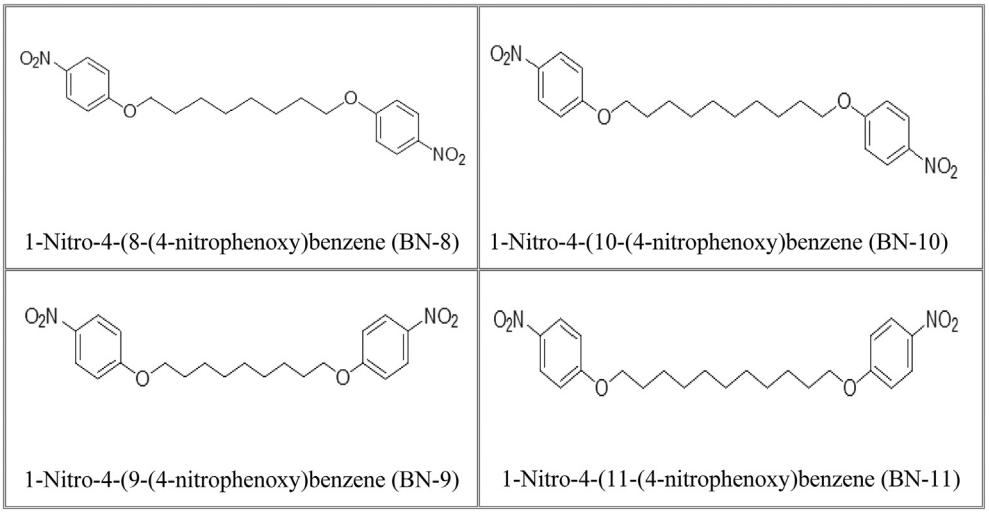

Figure 1. The structures of bisnitrophenoxy compounds (BN-8 to BN-11).

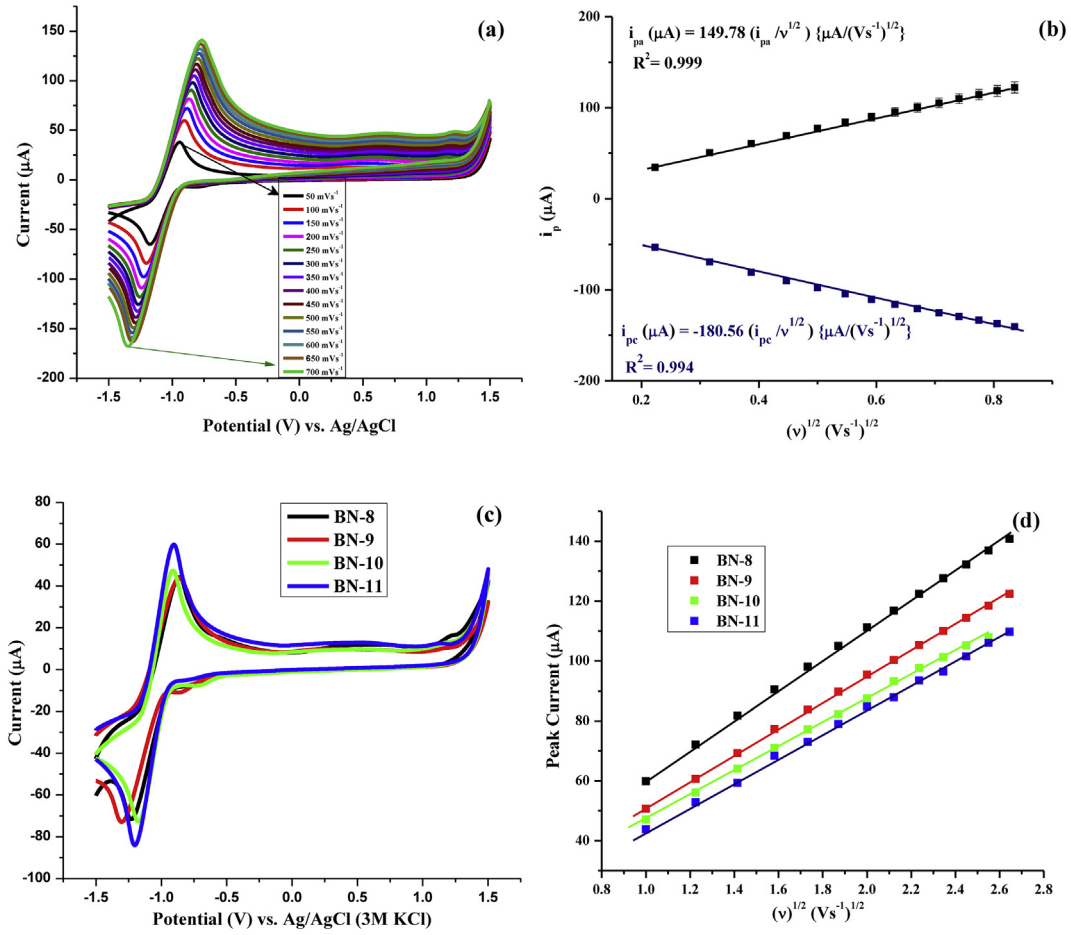

Figure 3. a) Effect of sweep rates on cyclic voltammetric responses of BN-8 at 50–700 mVs^{-1}, b) Linear regression plots of anodic and cathodic peak current values vs. $\nu^{1/2}$ for BN-8, c) Cyclic voltammograms of BN-8 to BN-11 (5 mM) at 100 mVs^{-1} and 298 K, d) Plot of $\nu^{1/2}$ versus I_p values for the determination of diffusion coefficients (D_o) of all compounds.

Table 1. Voltammetric parameters of bisnitrophenoxy compounds (BN-8 to BN-11) at 0.1 Vs^{-1}.

Compound	I_{pa} (μA)	I_{pc} (μA)	E^o (V)	ΔE_p (V)	I_{pc}/I_{pa}
BN-8	43.76	72.93	1.083	0.443	1.66
BN-9	47.06	74.54	1.048	0.377	1.59
BN-10	50.67	69.38	1.039	0.262	1.36
BN-11	59.82	84.06	1.053	0.298	1.40

* I_{pa} = oxidation current, I_{pc} = reduction current, E = formal potential, ΔE_p = difference in peak potentials.

Table 2. Electrochemical parameters of bisnitrophenoxy compounds at 0.1 Vs^{-1} and 298 K.

Compounds	Anodic Peak (E_p-$E_{p/2}$)/V	Cathodic Peak (E_p-$E_{p/2}$)/V	αn_a	αn_c
BN-8	0.104	-0.134	0.46	0.35
BN-9	0.096	-0.128	0.49	0.37
BN-10	0.122	-0.169	0.39	0.28
BN-11	0.134	-0.193	0.35	0.25

* (E_p-$E_{p/2}$) = 47.7/αn (mV) [37] was used to calculate 'αn' values for cathodic and anodic peaks.

Cyclic voltammetric profile of bisnitrocompounds revealed a couple of two peaks, reduction peak at -1.23 V and oxidation peak at -0.86 V. In Figure 2, the CV responses of GC in solvent mixture with (black line) and without bisnitrophenoxy compound (BN-8) (red line) are presented. The peak at -1.230 V was ascribed to the reduction potential of the nitro group. The voltammograms correlated with reported electrochemical (EC) mechanism (Eq. i & ii, Figure 2). These phenomena revealed two distinct redox peaks attributable to single electron reduction of the nitro group to form NO_2^- ion and consequent formation of the neutral species upon electrooxidation as presented [34, 35].

3.1.1. Estimation of diffusion coefficients (Do)

The diffusion coefficient values were estimated using cyclic voltammetric (CV) profiles and variation of peak current with scan rates (Figure 3). In these responses, a resemblance was observed in the voltammetric behavior of the compound and structural subtleties. The ratio of reduction and oxidation currents (I_{pc}/I_{pa}) was calculated for each response as a criterion to analyse the reversibility of the redox process and is given in Table 1. The voltammetric parameters for all bisnitrophenoxy compounds at 0.1 Vs^{-1} scan rates are given in Table 2, while the voltammetric responses with variation in scan rate are given in Figure 3a. At higher scan rates, another new peak around 1.2 V was observed at a more positive potential along with a clear peak shift.

Cyclic voltammetric measurements for all other bisnitrocompounds (BN-9, 10 and 11) offered a similar electrochemical trend under similar conditions of temperature and scans (Figure 3 (c). The tested bisnitrophenoxy compounds were all redox-active with the reversible electron transfer process. A linear increasing trend of I_p with $\nu^{1/2}$ was observed which demonstrated the mass transport process to be diffusion controlled confirmed from linear regression plot (Figure 3d). The value of peak current ratio, $I_{pc}/I_{pa} > 1$ (Table 1), also reflects the reversibility of redox process [36]. Therefore, one can apprehend from CV data that the electron transfer follows a reversible diffusion-controlled single electron transfer process corresponding to NO_2/NO_2^- redox couple [37]. Linear dependence of peak current values with the square root of scan rate can be described by the following equations;

$$I_{pa} = 149.78\left(I_{pa} \,/\, v^{1/2}\right)\left\{\mu A \,/\, \left(Vs^{-1}\right)^{1/2}\right\} \quad R^2 = 0.999 \tag{1}$$

$$I_{pc} = -180.56\left(I_{pc} \,/\, v^{1/2}\right)\left\{\mu A \,/\, \left(Vs^{-1}\right)^{1/2}\right\} \quad R^2 = 0.994 \tag{2}$$

These trends indicate the facility of $ArNO_2/ArNO_2^-$ redox process in aprotic solvent.

3.1.2. Determination of reaction rate

The heterogeneous rate constant ($k_{s,h}$) was evaluated by Gileadi's method by using the values of diffusion coefficients and critical scan rates (ν_c) [38]. Critical scan rate was estimated by plotting the logarithm of scan rate against E_p at a particular temperature. The obtained plots revealed a linear trend, with two distinctive regions, one having low value of slopes observed at relatively lower scan rates however, the second one with greater slope at higher scan rates. The point where two lines intersect is called 'toe' which corresponds to critical scan rate value (ν_c). By applying Eq. (3), ν_c values were used to determine the heterogeneous rate constants, $k_{s,h}$ (Table 3).

$$\log k_{s,h} = -0.48\alpha + 0.52 + \log\left[\frac{nF\alpha\nu_c D_\circ}{2.303RT}\right]^{1/2} \tag{3}$$

Where, D_o represents the diffusion coefficient of the nitro group (electrophore) and α is the dimensionless parameter called transfer coefficient with other usual parameters. However, values of charge transfer coefficient (α) were determined by the application of Kochi method [39]:

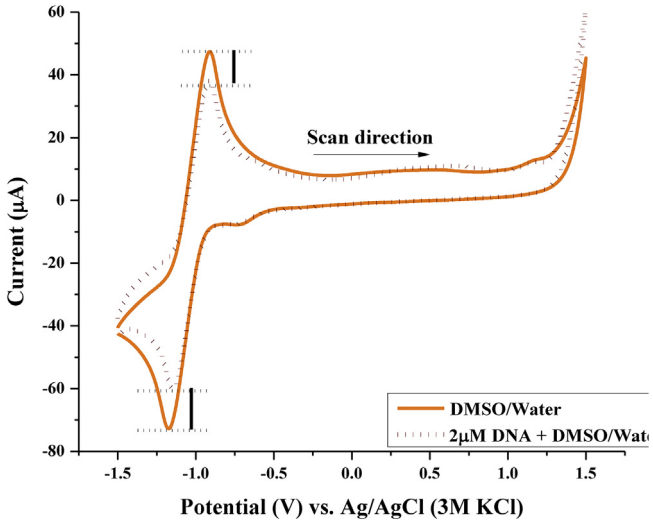

Figure 4. Decrease in current (anodic and cathodic) signal with the addition of dsDNA, observed for BN-8 compound in DMSO/water binary mixture at 0.1 Vs^{-1}.

$$\alpha = \frac{\left(E_{\frac{1}{2}} - E_C\right)}{E_p^a - E_p^c} \tag{4}$$

The results revealed that the molecular size and CH_2 group significantly affects the heterogeneous rate constant values. With the increase in CH_2- chain length, a corresponding decrease in the rate constant values was observed. These observations could be correlated with the smaller size, greater mobility and higher diffusion constants. It is inferred that the diffusion constant decreased with the incorporated methylene units which lowered the mobility of nitrophenoxy compounds and diminished their diffusion constant values [40].

3.2. DNA interaction studies using cyclic voltammetry

Cyclic voltammograms were recorded for fixed concentration (5 mM) of bisnitrophenoxy compounds in the potential window of -1.5 to 1.5 V with sequential addition of dsDNA (2–26 μM) at 298 K and 0.1 V s^{-1}. The substantial decrease in current for both oxidation and reduction peaks were observed which is an indicative of intercalative interaction of planar part of compound (Figure 4), also pointing towards the diminution in the amount of unbound nitrocompound [9].

The interaction of BN-8 with dsDNA can be inferred from the slight shift in peak position and decrease in peak height, as shown in Figure 5. After subsequent addition of dsDNA, a saturation point is reached which can be estimated by the percent decrease in peak current, %Δ*I* which indicates the influence of spacer length upon bisnitrophenoxy compound-dsDNA interactions. %Δ*I* for these compounds (BN-8 to BN-11) was calculated using Eq. (5).

$$\%\Delta I = \frac{(I_P - I_{Po})}{I_{po}} \times 100 \tag{5}$$

Table 3. Kinetic parameters for N-bisnitrophenoxy compounds at 298 K.

Compounds	α	ν_c	Heterogeneous rate constant, $k_{s,h}$ x 10^{-3} (cms^{-1})
BN-8	0.30	0.36	5.93
BN-9	0.34	0.32	4.88
BN-10	0.65	0.30	4.28
BN-11	0.64	0.34	4.39

$k_{s,h}$ varies in the order: BN-8 > BN-9 > BN-10 > BN-11.

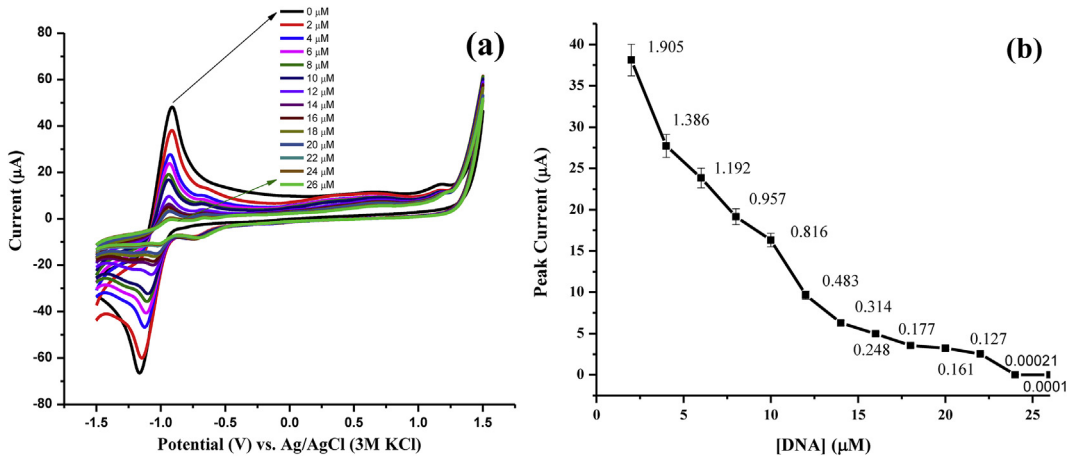

Figure 5. a) Cyclic voltammetric response for BN-8 (5 mM) in different concentrations of dsDNA b) Decreasing peak current trend with the dsDNA concentrations along with standard errors.

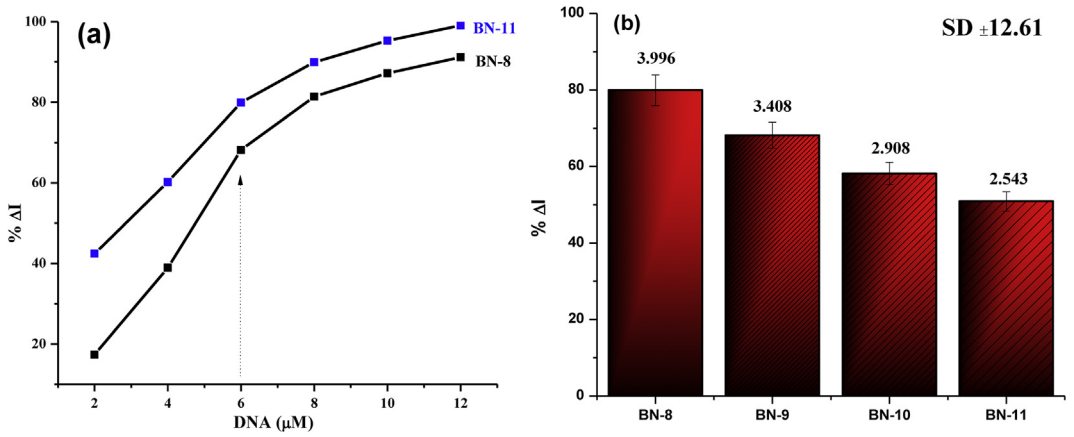

Figure 6. a) A plot of %decrease in peak current with sequential addition of dsDNA (2–12 μM) for BN-8 and BN-11, b) Bar diagram representing the standard errors and standard deviation in %ΔI values for optimal concentration of dsDNA.

Where, I_{Po} and I_P are the peak current values with and without dsDNA. An increase in %Δ*I* was observed with the addition of dsDNA. However, after a certain optimal amount of dsDNA (6 μM), the trend in %Δ*I* showed a constant deviation. The substantial reduction in peak current is due to the formation of heavy BN-dsDNA adduct, which results in the lowering of free concentration of the electrophore, N. The observed %ΔI trend for bisnitroaromatic compound is; BN-8 (50.86) ˂ BN-9 (58.17) ˂ BN-10 (68.16) ˂ BN-11 (19.93) (Figure 4). Diffusion coefficient values for compound-dsDNA adduct were much smaller than those for the free compounds, as expected.

Threading intercalation (intercalation + groove-binding) could be the reason for the maximum value of %ΔI observed for BN-11 compound (Figure 6). This mixed mode of binding is strongly dependent on the relative increase in molecular size and spacer chain-length of bisnitrophenoxy compounds [9]. BN-11 has a greater number of methylene spacer groups, therefore it has a maximum capacity of threading intercalation and hence, binds more strongly with dsDNA as compared to bisnitrophenoxy compounds possessing smaller chains.

3.2.1. Estimation of diffusion rates

In order to quantify the interaction of compounds with dsDNA, CV studies were carried out at 0.1 Vs^{-1} scan rate and diffusion coefficients were calculated using Randles-Sevcik equation [9, 41].

$$I_p = 2.69 \times 10^5 (n)^{3/2} A C_o {}^* D_o^{1/2} \nu^{1/2} \quad (6)$$

Where, I_p represents the peak current (A), n is the charge-transfer number, A is the area of electrode (cm^2), $C_o{}^*$ is the concentration (mol cm^{-3}), D_o is the diffusion coefficient ($cm^2\ s^{-1}$) and ν is the scan rate (Vs^{-1}). The slope 0.5 corresponds to diffusion-controlled process when plotted in a logarithmic form (log I_p vs. log ν). With the addition of dsDNA, a linear decrease in diffusion coefficient values was observed as shown in Tables 4 and 5.

Upon titration of compounds with dsDNA, a gradual decrease in diffusion coefficient values was observed, a comparison for all compounds is presented in Figure 7 (b). However, upon addition of more dsDNA into the fixed concentration of bisnitrophenoxy compound, there is an increase in intercalative interactions, that results in increased dsDNA-bound compound and a diminution in the amount of free electroactive species.

In the present study, results demonstrated the effect the additional spacer length and sizes of symmetrical molecules on D_o values, showing a decreasing order. This corresponds well to the recent reports, where D_o values of electro-reduction products for various substituted nitroaromatics varied linearly with their molecular structure and sizes [42].

A comparison of kinetic parameters is presented in the form of bar diagram in Figure 7 (a) illustrating the decrease in parameters in increased size providing more hindrance to the electron transfer process.

3.2.2. Binding parameters for BN-dsDNA adduct

Interacalation of small molecules with biological macromolecules results in the formation of a complex, and the extent of binding can be

Table 4. Diffusion coefficient values of neat bisnitrophenoxy compounds.

Compounds	D_o x 10^{-6} (cm^2s^{-1})	Standard error
BN-8	3.41	±0.87
BN-9	2.50	±1.38
BN-10	2.13	±1.04
BN-11	1.97	±0.61

Table 5. Diffusion coefficient values for BN-8 with the addition of dsDNA concentrations.

dsDNA (μM)	(D_o x 10^{-7}/cm^2 s^{-1})
0.00	3.41
2.00	2.59
4.00	2.45
6.00	1.98
8.00	1.56
10.00	1.10

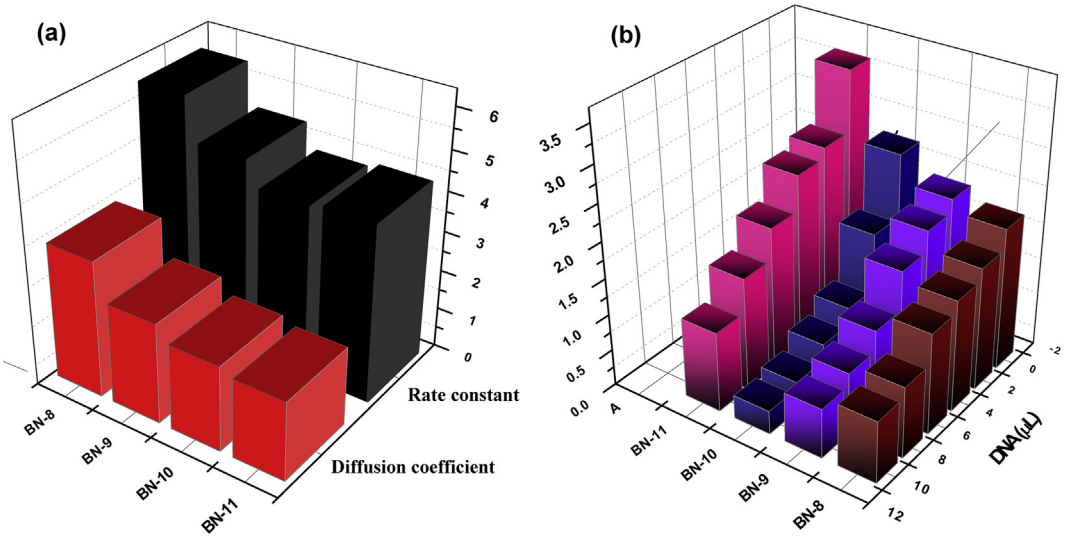

Figure 7. Representation of (a) kinetic parameters for bisnitroaromatic compounds in the form of 3D bar graph (b) estimated diffusion coefficients for free and BN-dsDNA bound complexes.

studied by binding or formation constants K_b (M^{-1}) of macromolecule adduct with guest compounds. Thermodynamic studies of this complex can be used to determine binding constant. Eq. (7) can be used to calculate the binding constants of bisnitroaromatic compounds-dsDNA complex using peak current values [43]. Binding constant can be determined from the reciprocal of slope of Ip^2 versus $Ip_o^2 - Ip^2/[dsDNA]$ plot, which gives the straight line when there is excess amount of compound is available with less or no dsDNA (Figure 8a).

$$I_p^2 = \frac{1}{K_b[dsDNA]}\left(I_{p_o}^2 - I_p^2\right) + I_{p_o}^2 - [dsDNA] \tag{7}$$

The order of binding constants of bisnitroaromatic compound-dsDNA complexes evaluated by voltammetric studies is found to be;

BN-8 < BN-9 < BN-10 < BN-11

The calculated highest value of K_b for BN-11 (Table 6) also indicated the enhanced binding and formation of most stable compound-DNA complex.

The Gibbs free energy equation (Eq. 8) and formation constant data (Table 6) were used to evaluate ΔG and the obtained values are given in Table 6.

$$\Delta G\ (\mathrm{kJmol^{-1}}) = -\mathrm{RTlnK_b} \tag{8}$$

The order of magnitude of ΔG values increases slightly with the respective structure of each bisnitrophenoxy compound. Thermodynamic studies also corresponded to CH_2-spacer in the structures and pointed to stronger binding of BN-11 with dsDNA as compared to BN-8. The binding of dsDNA with bisnitrocompounds is a spontaneous process, as evident from the negative values of ΔG [44].

Binding site sizes are another parameter to check the binding affinity of compounds with dsDNA. During intercalation, the guest molecules interact with available dsDNA base pairs, these available sites are termed as binding sites. Binding site size (s) per base pairs of dsDNA was calculated by using the following equations [43, 45];

$$\frac{C_b}{C_f} = K_b\{[dsDNA] \Big/ 2s\} \tag{9}$$

Where, C_f is the concentration of free bisnitrophenoxy and C_b is the concentration of BN-dsDNA adduct. Eq. (10) was used to determine this ratio which is given as;

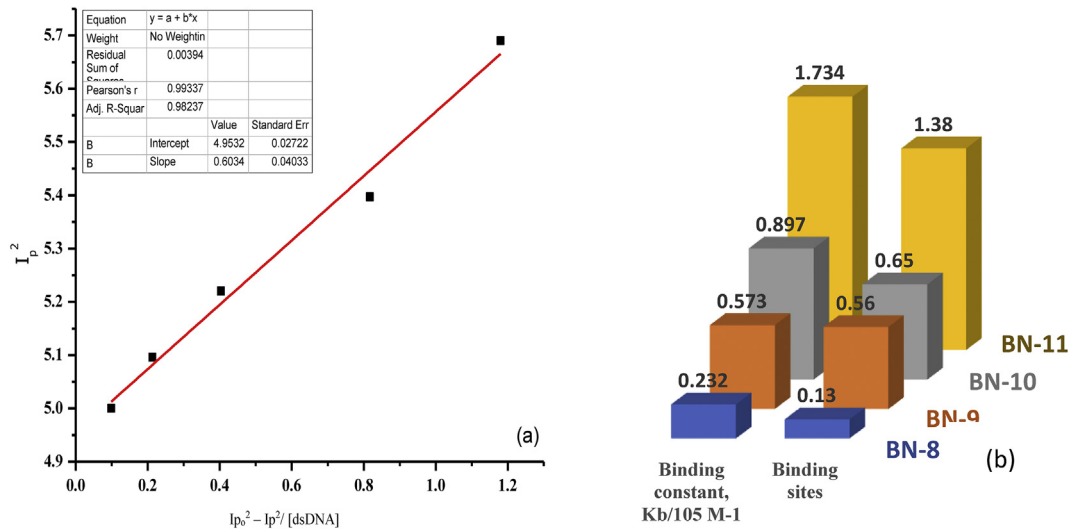

Figure 8. (a) Functional plot of Ip vs. Ip_o^2 -Ip^2/[dsDNA] for the estimation of K_b of BN-8, (b) graphical representation of increased binding sites and binding constants with increase CH_2- length in molecular structure.

Table 6. Calculated binding parameters for BN-dsDNA interaction.

Compounds	Binding constant $K_b/10^4$ M^{-1}	Gibbs free energy $-\Delta G$/kJ mol^{-1}	Binding sites
BN-8	2.32	24.89	0.13
BN-9	5.73	27.73	0.56
BN-10	8.97	28.24	0.65
BN-11	17.34	29.87	1.38

$$\frac{C_b}{C_f} = \frac{I - I_{DNA}}{I_{DNA}} \quad (10)$$

The number of these site sizes in dsDNA bound bisnitrophenoxy complex has shown an increasing trend with the size of guest compound [42, 43].

Order of increasing binding sites and binding constants indicates the enhanced threading intercalation ability of BN-11 compound, data is tabulated in Table 6 and graphically presented in Figure 8b. Threading mode of intercalation was inferred from the observed data as well as corresponding symmetrical structures of bisnitrophenoxy compounds under study, which consist of both the hydrophobic and the hydrophilic parts necessary for threading intercalation which is actually wrapping of dsDNA by combined effect of intercalation and groove-binding favored by planar and nonplanar features in small chained molecular configurations [46].

4. Conclusions

Cyclic voltammograms of bisnitrocompounds (BN-8, BN-9, BN-10, BN-11), with different molecular chain lengths, recorded in argon saturated binary mixture of DMSO and water in potential range of -1.5 to 1.5 V at 298 K showed their redox activity with the reversible single electron transfer process. Bisnitrocompounds were all redox active and results demonstrated the diffusion-controlled nature of charge transfer process occurring at the electrode surface corresponding to $ArNO_2/ArNO_2^-$ redox couple. Order of decreasing diffusion rates, D_o (10^{-6} cm^2s^{-1}) with increasing molecular size, is BN-8 (3.41) > BN-9 (2.50) > BN-10 (2.13) > BN-11 (1.97). Gileadi's method was used to estimate the heterogeneous rate constant values ($k_{s,h}$), which also depicted the effect of molecular size and CH_2 group on the kinetic parameters. The increase in chain length influence the rate constant and diffusion coefficient values, thus rendering the process to be diffusion-controlled. An eminent decrease in signal with the slight shift in peak position after subsequent addition of dsDNA, inferred the interaction of bisnitroaromatic compound with dsDNA. Observed values of binding or formation constants specifies the good binding ability of bisnitrophenoxy compounds with DNA. The maximum binding sites (1.38) was observed for 1-nitro-4-(-11-(-4-nitrophenoxy)undecyloxy)benzene (BN-11), which pointed towards the enhanced threading intercalation with the increased molecular size. The molecular signatures as longer chains in bisnitrocompounds compounds can be further investigated as potential drugs for dsDNA binding.

Declarations

Author contribution statement

Maria Shakeel, Tehmeena Maryum Butt, Maria Zubair, Humaira Masood Siddiqi, Naveed Kauser Janjua, Zareen Akhter: Conceived and designed the experiments; Performed the experiments; Analyzed and interpreted the data; Contributed reagents, materials, analysis tools or data; Wrote the paper.

Azra Yaqub, Sadia Mahmood: Performed the experiments.

Funding statement

This work was supported by the Quaid-i-Azam University Islamabad and Higher Education Commission (HEC) Pakistan (research grant No. 10-1718).

Competing interest statement

The authors declare no conflict of interest.

Additional information

No additional information is available for this paper.

Acknowledgements

Dr. Ayesha Mujtaba is acknowledged for the proof-reading and some calculations, (ayesha.mujtaba@live.com).

References

[1] W. Guschlbauer, in: DNA-ligand Interactions: from Drugs to Proteins, 137, Springer Science & Business Media. Plenum press, New York and London, 2013, pp. 113–126.
[2] A. Buschini, L. Ferrarini, S. Franzoni, S. Galati, M. Lazzaretti, F. Mussi, C. Northfleet de Albuquerque, T. Maria Araújo Domingues Zucchi, P. Poli, Genotoxicity revaluation of three commercial nitroheterocyclic drugs: nifurtimox, benznidazole, and metronidazole, Journal of Parasitol Res 2009 (2009) 11.
[3] A.M. Havelka, M. Berndtsson, M.H. Olofsson, M. C Shoshan, S. Linder, Mechanism of action of DNA-damaging anticancer drugs in treatment of carcinomas: is acute apoptosis an "off-target" effect? Mini Rev. Med. Chem. 7 (2007) 1035–1039.
[4] Q. Li, W. Xu, Novel anticancer targets and drug discovery in post genomic age, Curr. Med. Chem. Anti Cancer Agents 5 (2005) 53–63.
[5] A. Kamal, D.R. Reddy, M.K. Reddy, G. Balakishan, T.B. Shaik, M. Chourasia, G.N. Sastry, Remarkable enhancement in the DNA-binding ability of C_2-fluoro substituted pyrrolo [2, 1-c][1, 4] benzodiazepines and their anticancer potential, Bioorg. Med. Chem. 17 (2009) 1557–1572.
[6] M. Sirajuddin, S. Ali, V. McKee, M. Sohail, H. Pasha, Potentially bioactive organotin (IV) compounds: synthesis, characterization, in vitro bioactivities and interaction with SS-DNA, Eur. J. Med. Chem. 84 (2014) 343–363.
[7] A. Rescifina, C. Zagni, M.G. Varrica, V. Pistarà, A. Corsaro, Recent advances in small organic molecules as DNA intercalating agents: synthesis, activity, and modeling, Eur. J. Med. Chem. 74 (2014) 95–115.
[8] W.H. Chen, J.Y. Pang, Y. Qin, Q. Peng, Z. Cai, Z.H. Jiang, Synthesis of linked berberine dimers and their remarkably enhanced DNA-binding affinities, Bioorg. Med. Chem. Lett 15 (2005) 2689–2692.
[9] N.K. Janjua, Z. Akhter, F. Jabeen, B. Iftikhar, Cyclic voltammetric investigation of interactions between bisnitroaromatic compounds and ds. DNA, J. Kor. Chem. Soc. 58 (2014) 153–159.
[10] R.A. Hutchins, J.M. Crenshaw, D.E. Graves, W.A. Denny, Influence of substituent modifications on DNA binding energetics of acridine-based anticancer agents, Biochem 42 (2003) 13754–13761.
[11] Y.H. Long, L.P. Bai, Y. Qin, J.Y. Pang, W. H Chen, Z. Cai, Z.L. Xu, Z.H. Jiang, Spacer length and attaching position-dependent binding of synthesized protoberberine dimers to double-stranded DNA, Bioorg. Med. Chem. 14 (2006) 4670–4676.
[12] U. Tawar, A.K. Jain, B. Dwarakanath, R. Chandra, Y. Singh, N. Chaudhury, D. Khaitan, V. Tandon, Influence of phenyl ring disubstitution on bisbenzimidazole and terbenzimidazole cytotoxicity: synthesis and biological evaluation as radioprotectors, J. Med. Chem. 46 (2003) 3785–3792.
[13] M. Godzieba, S. Ciesielski, Natural DNA intercalators as promising therapeutics for cancer and Infectious diseases, Curr. Cancer Drug Targets 20 (2020) 19–32.
[14] D.R. Boer, L. Wu, P. Lincoln, M. Coll, Thread insertion of a Bis (dipyridophenazine) diruthenium complex into the DNA double helix by the extrusion of AT base pairs and cross-linking of DNA duplexes, Angew. Chem. Int. Ed. 53 (2014) 1949–1952.
[15] J. Squella, S. Bollo, L. Nueez Vergara, Recent developments in the electrochemistry of some nitro compounds of biological significance, Curr. Org. Chem. 9 (2005) 565–581.
[16] G.D.M.C. Perdigão, M.S. Lopes, L.B. Marques, P.H.D.M. Prazeres, K. de Sousa Gomes, R.B. de Oliveira, E.M. De Souza-Fagundes, Novel nitroaromatic compound activates autophagy and apoptosis pathways in HL60 cells, Chem. Biol. Interact. 283 (2018) 107–115.
[17] M.L. Nigro, A. Palermo, M. Mudry, M. Carballo, Cytogenetic evaluation of two nitroimidazole derivatives, Toxicol. Vitro 17 (2003) 35–40.
[18] X. Jiang, X. Lin, Voltammetry of the interaction of metronidazole with DNA and its analytical applications, Bioelectrochemistry 68 (2006) 206–212.
[19] C.M. Aravena, R. Figueroa, C. Olea-Azar, V.J. Aran, Electrochemical and ORAC studies of nitro compounds with potential antiprotozoal activity, J. Chilian Chem. Soc. 55 (2010) 244–249.
[20] J.E. Biaglow, B. Jacobson, C.L. Greenstock, J. Raleigh, Effect of nitrobenzene derivatives on electron transfer in cellular and chemical models, Mol. Pharmacol. 13 (1977) 269–282.
[21] A. Gooch, N. Sizochenko, L. Sviatenko, L. Gorb, J. Leszczynski, A quantum chemical based toxicity study of estimated reduction potential and hydrophobicity in series of nitroaromatic compounds, SAR QSAR Environ. Res. 28 (2017) 133–150.
[22] N. Shahabadi, M. Maghsudi, Multi-spectroscopic and molecular modeling studies on the interaction of antihypertensive drug; methyldopa with calf thymus DNA, Mol. Biosyst. 10 (2014) 338–347.
[23] G.Y. Wang, C. Song, D.M. Kong, W.J. Ruan, Z. Chang, Y. Li, Two luminescent metal–organic frameworks for the sensing of nitroaromatic explosives and DNA strands, J. Mat. Chem. A. 2 (2014) 2213–2220.
[24] M. Arkin, E. Stemp, C. Turro, N. Turro, J. Barton, Luminescence quenching in supramolecular systen: a comparison of DNA and SDS micelle-mediated photoinduced electron transfer between metal complexes, J. Am. Chem. Soc. 118 (1996) 2267–2274.
[25] K. Sandström, S. Warmlander, M. Leijon, A. Gräslund, 1H NMR studies of selective interactions of norfloxacin with double-stranded DNA, Biochem. Biophys. Res. Commun. 304 (2003) 55–59.
[26] M. Montazerozohori, M. Sedighipoor, Synthesis, spectral identification, electrochemical behavior and theoretical investigation of new zinc complexes of bis ((E) 3-(2-nitrophenyl)-2-propenal) propane-1, 2-diimine, Spectrochim. Acta, Part A 96 (2012) 70–76.
[27] B. Horrocks, Functionalised monolayer for nucleic acid immobilisation on gold surfaces and metal complex binding studies, Anal 123 (1998) 753–757.
[28] J. Carbajo, S. Bollo, L.J. Nunez Vergara, P. Navarrete, J. Squella, Voltammetric studies of aromatic nitro compounds: pH-dependence on decay of the nitro radical anion in mixed media, J. Electroanal. Chem. 494 (2000) 69–76.
[29] A. Haider, Z. Akhter, F. Jabeen, N.K. Janjua, M. Bolte, Synthesis, structure and DNA binding studies of 1, 4-bis ((4-nitrophenoxy)methyl) benzene and its reduction derivative, J. Mol. Struct. 994 (2011) 242–247.
[30] P. Vidlakova, H. Pivonkova, M. Fojta, L. Havran, Electrochemical behavior of anthraquinone-and nitrophenyl-labeled deoxynucleoside triphosphates: a contribution to development of multipotential redox labeling of DNA, Monatshefte für Chemie-Chemical Monthly 146 (2015) 839–847.
[31] M. Montazerozohori, M. Sedighipoor, S. Joohari, Electrochemical behavior of bis ((E) 3-(2-nitrophenyl) allylidene) propane-1, 2-diamine as a new schiff base and some its new XII group complexes, Int. J. Electrochem. 7 (2012) 77–88.
[32] M.S.U. Khan, Z. Akhter, T. Naz, A.S. Bhatti, H.M. Siddiqi, M. Siddiq, A. Khan, Study on the preparation and properties of novel block copolymeric materials based on structurally modified organometallic as well as organic polyamides and polydimethylsiloxane, Polym. Int. 62 (2013) 319–334.
[33] M. Shakil, T. Akhter, H.M. Siddiqi, Z. Akhtar, The effect of even-odd methylene spacer groups on the thermal stability of epoxy-amine polymers, J. Chem. Soc. Pakistan 37 (2015) 92–98.
[34] A. Alvarez-Lueje, H. Pessoa, L.J. Nunez Vergara, J.A. Squella, Electrochemical reduction of 2, 5-dimethoxy nitrobenzenes: nitro radical anion generation and biological activity, Bioelectrochem. Bioenerg. 46 (1998) 21–28.
[35] S. Bollo, L.J. Nunez Vergara, J. Squella, Cyclic voltammetric determination of free radical species from nitroimidazopyran: a new antituberculosis agent, J. Electroanal. Chem. 562 (2004) 9–14.
[36] F.R. Paula, G.H. Trossini, E.I. Ferreira, S.H. Serrano, C. Menezes, L.C. Tavares, Theoretical and voltammetric studies of 5-nitro-heterocyclic derivatives with potential trypanocidal activities, J. Braz. Chem. Soc. 21 (2010) 740–749.
[37] A.J. Bard, L.R. Faulkner, J. Leddy, C.G. Zoski, in: Electrochemical Methods: Fundamentals and Applications, 2, Wiley, New York, 1980, p. 482.
[38] U. Eisner, E. Gileadi, Anodic oxidation of hydrazine and its derivatives: Part I. The oxidation of hydrazine on gold electrodes in acid solutions, J. Electroanal. Chem. Interfacial Electrochem. 28 (1970) 81–92.
[39] R.J. Klingler, J.K. Kochi, Electron-transfer kinetics from cyclic voltammetry; quantitative description of electrochemical reversibility, J. Phys. Chem. 85 (1981) 1731–1741.
[40] G. Zhang, J. Guo, J. Pan, X. Chen, J. Wang, Spectroscopic studies on the interaction of morin–Eu (III) complex with calf thymus DNA, J. Mol. Struct. 923 (2009) 114–119.
[41] J.E. Randles, A cathode ray polarograph. Part II.—the current-voltage curves, Trans. Faraday Soc. 44 (1948) 327–338.
[42] D.P. Valencia, F.J. Gonzalez, Estimation of diffusion coefficients by using a linear correlation between the diffusion coefficient and molecular weight, J. Electroanal. Chem. 10 (2012) 121–126.
[43] M. Aslanoglu, Electrochemical and spectroscopic studies of the interaction of proflavine with DNA, Anal. Sci. 22 (2006) 439–443.
[44] J.H. Shi, D.Q. Pan, K.L. Zhou, Y. Lou, Exploring the binding interaction between herring sperm DNA and sunitinib: insights from spectroscopic and molecular docking approaches, J. Biomol. Struct. Dyn. 37 (2019) 837–845.
[45] M.T. Carter, M. Rodriguez, A.J. Bard, Voltammetric studies of the interaction of metal chelates with DNA, 2. tris-chelated complexes of cobalt (III) and iron (II) with 1, 10-phenanthroline and 2, 2'-bipyridine, J. Am. Chem. Soc. 111 (1989) 8901–8911.
[46] R. Hajian, M. Tavakol, Interaction of anticancer drug methotrexate with ds-DNA analyzed by spectroscopic and electrochemical methods, J. Chem. 9 (2012) 471–480.